Magnetic Frustration and Anisotropy in High-T_C Iron Pnictides

Myung Joon Han, Quan Yin*, Warren E. Pickett, and Sergey Y. Savrasov
Department of Physics, University of California, Davis, California 95616, USA
(Dated: November 4, 2008)

Using first-principle density functional theory calculations combined with tight-binding method, dynamical mean field theory, and linear response theory, we extensively investigated the electronic structures and magnetic interactions of nine ferropnictides representing three different structural classes. The calculated magnetic interactions are found to be short-range, and the nearest (J_{1a}) and next-nearest (J_2) exchange constants follow the universal trend of $J_1/2J_2 \sim 1$, despite their extreme sensitivity to the z-position of As. This suggests magnetic frustration as the key factor in stabilizing the superconducting ground state. The calculated spin wave dispersions show strong magnetic anisotropy in the Fe plane, in contrast to cuprates.

PACS numbers: 74.70.-b, 71.18.+y, 71.20.-b, 75.25.+z

Recent discovery of the new high-temperature superconductor, $LaO_{1-x}F_xFeAs$ with a transition temperature (T_C) of $26K$ [1] has triggered tremendous research activities on iron pnictides. Rare-earth (RE) doping increases T_C up to $55K$ for Sm [2, 3]. Replacing RE-O layers with Li produces an intrinsic superconductor LiFeAs with T_C of $18K$ [4]. The 122 ferropnictides, $AL Fe_2As_2$ (AL: Ca, Sr, Ba, K), span another structural class with T_C up to $38K$ [5, 6, 7, 8, 9, 10]. More recently, arsenic-free $FeSe_{1-\delta}$ and $Fe(Se_{1-x},Te_x)_{1-\delta}$ without any interlayer between Fe-(Se,Te) planes were found to be superconducting at T_C as high as $27K$ under pressure [11, 12, 13, 14]. In spite of the accumulating reports of both experiments and theories, the nature of the superconductivity and magnetism is still far from clear. After several works have ruled out the phonon-electron coupling [15, 16], and the coexistence of magnetic fluctuation and superconductivity being confirmed by μSR [17], intensive investigations have been focused on the magnetic properties of these systems [18, 19, 20, 21, 22, 23, 24, 25]. From the studies up to now, one of the common and evident features is the interplay between superconductivity and magnetism. It is clear, from the different structures, that the essential physics lies in the iron plane forming the 2-dimensional spin lattice.

Except for the Fe(Se,Te) family suggested to have different magnetic structures by recent studies [18, 19, 20], it is generally believed that the first three classes of Fe pnictides have the same superconducting mechanism closely related to magnetic interactions. In order to clarify the raised issues and lead to further understanding, it is of key importance to investigate the exchange interactions across different classes of compounds and examine any trend or common features. However, material-specific information of magnetic interactions is scarce in spite of active research activities. The direct probe of spin dynamics is inelastic neutron scattering, which has been recently performed for $SrFe_2As_2$ [9] and $CaFe_2As_2$ [26]. They have revealed that the combination of nearest and next nearest neighbor exchange interactions $|J_{1a} + 2J_2|$ is about $100meV$, but detailed data from individual contributions, as well as their anisotropy and the proximity of the ratio $J_{1a}/2J_2$ to the critical value of 1, which has been discussed extensively in recent publications [21, 22, 23], are still missing.

In this Letter, using first-principles linear response calculations [27, 28], we provide the data of in-plane magnetic exchange interactions for several Fe-based superconductors, and discuss their spin wave dispersions. The data suggest that magnetic fluctuation plays an important role. A total of nine materials have been studied: REFeAsO (RE: La, Ce, Pr, Nd), $AL Fe_2As_2$ (AL: Ca, Sr, Ba, K), and LiFeAs. Exchange interactions of these systems are found to be short-range despite of their metallic density-of-states (DOS), and the calculated interaction strengths follow the universal behavior of $J_{1a} \approx 2J_2$ for all materials, which corresponds to the frustrated magnetic structure [21, 22, 23]. Considering not only the variety of the materials studied here but also the high sensitivity of the Fe moment to the z-position of As atom [29, 30], this universal behavior of the exchange interactions is impressive, and it suggests that magnetic fluctuation may be the key factor stabilizing the superconducting ground state in the Fe-based high T_C superconductors. The calculated spin-wave dispersion shows an anisotropic spin interaction which is different from the cuprates.

There have been several published tight-binding (TB) parametrizations of the electronic structure of prototypical LaOFeAs in the vicinity of the Fermi level using fits based either on Wannier functions or atomic basis sets [31, 32, 33, 34]. However the current situation still looks complicated because the projected DOS deduced from electronic structure calculations are based on the spherical harmonic projectors within the atomic spheres that may not be very well suited for the extended Fe and As orbitals presented here. Due to these complications even the crystal field splitting of Fe d level appears to be controversial in the current literature [31, 32, 33, 34].

To better understand the complicated electronic structure around Fermi level, we performed TB analysis by considering d_{xz} and d_{yz} orbitals of Fe t_{2g} manifold hybridizing with the arsenic p_x and p_y, respectively. As shown in Fig. 1, the separation between the energy levels

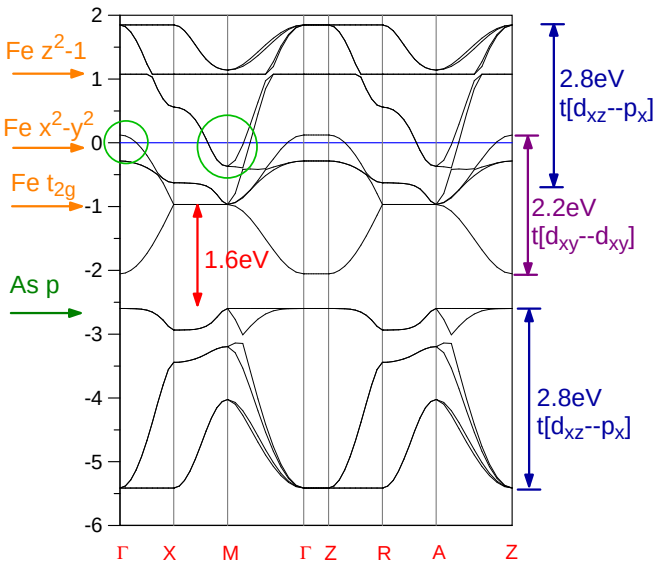

FIG. 1: (Color online) Tight-biding the band structure of LaFeAsO. The circles at the Fermi level on the Γ and M points indicate the hole and electron pockets, respectively.

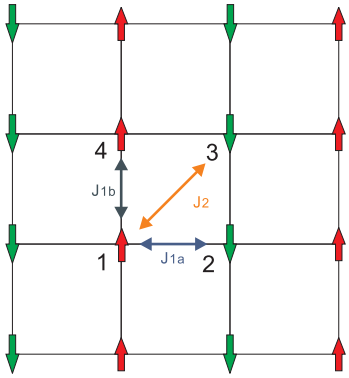

FIG. 2: (Color online) Spin arrangment and exchange interactions in the Fe plane of the striped Q_m-AFM phase. The arrows on lattice sites indicate the Fe spin directions. The double arrows indicate the nearest neighbor AFM interaction (J_{1a}), FM interaction (J_{1b}) and next nearest neighbor AFM interaction (J_2).

of Fe-t_{2g} and As-$p_{x,y}$ states is about $1.6eV$. Accounting for the hybridization matrix element between d_{xz}-p_x , d_{yz}-p_y states, which is of the order of $1.8eV$, produces bonding and antibonding bands, both having the bandwidth of $2.8eV$ with the Fermi level falling into the antibonding part of the spectrum (approximately $1eV$ above the Fe t_{2g} level). We also take into account the d_{xy} state of Fe which hybridizes with itself (hopping integral is approximately $0.3eV$), which produces an additional bandwidth of $2.2eV$. The resulting bandwidth of Fe d-electron character near the Fermi level becomes $2.8 + 2.2/2 = 3.9eV$ as exactly seen in the LDA calculation [35]. The coordinate system used here is the original crystallographic lattice where the spin alternates in the (π, π) direction. In this picture, the Γ-centered hole pockets (small circle in Fig. 1) are mostly of d_{xy} character, and the M-centered pockets (large circle) are of d_{xz}, d_{yz} character. This picture can be fine-tuned further by including the $d_{x^2-y^2}$ state which lies $0.3eV$ below the Fermi level and hybridizes primarily with As-$p_{x,y}$ states (hopping integral is about $0.8eV$) as well as hybridization between $d_{xz,yz}$ orbitals with As p_z states (hopping integral is about $0.4eV$). Note that in this picture the Fe d_{z^2-1} orbital becomes unoccupied and lies $1eV$ above the Fermi level.

Now we discuss the exchange interactions. To calculate the interactions between Fe moments, we used linear response theory [36, 37] based on first-principle density functional theory (DFT) calculations, which has been successfully applied to the $3d$ transition-metal oxides and the $5f$ actinides metallic alloys [37, 38]. We used the full potential linearized muffin-tin orbital (LMTO) as the basis set [39] and local spin density approximation (LSDA) for the exchange-correlation (XC) energy functional. Lattice constants are taken from experiments, and we performed the calculations at various $z(As)$, including experimental $z(As)_{\rm exp}$ and LDA optimized $z(As)_{LDA}$. In the calculations of REOFeAs compounds, we used the LSDA+DMFT method [27, 28] in which the RE $4f$ orbitals are treated as the localized ones within Hubbard I approximation. $U = 6eV$ and $J_H = 0.86eV$ were used as the on-site Coulomb repulsion and Hund's rule exchange parameter.

Fig. 2 shows the spin structure of the Fe plane which is common to the all magnetic Fe-based materials. Here we use the $(\pi, 0)$ striped AFM coordinate system, which is consistent with the ALFeAs class of materials and convenient to disscuss the spin wave dispersions. Magnetic interactions between Fe moments are governed by two dominating AFM couplings J_{1a} and J_2, and the FM nearest-neighbor exchange J_{1b} is small. We found the exchange interactions are of a short-range nature, whose q-dependence is well fitted by short-range exchange constants. This entitles us to discuss the competition of AFM spin interactions and magnetic frustration in the similar way adopted by the previous studies based on spin Hamiltonians assuming the local moment limit [21, 22, 23]. The results do not necessarilly conflict with the itinerant magnet picture because although the Fe $3d$ orbital has finite DOS at the Fermi level, the magnetic interactions can still remain short range, which possibly reflects the bad metallicity and some correlation (near Mott-insulator).

The calculated Fe magnetic moments and exchange interactions are summarized in Table I. We use the convention that positive J means AFM interaction. The calculated moments are consistent throughout the materials. The calculations done at experimental $z(As)_{\rm exp}$ are known to predict the moments about twice as large as experimental values, while at optimized $z(As)_{LDA}$ they

System	Moment	J_{1a}	J_2	J_{1b}	$J_{1a}/2J_2$	$J_{1a}+2J_2$
LaFeAsO	1.69	47.4	22.4	−6.9	1.06	92.2
CeFeAsO	1.79	31.6	15.4	2.0	1.03	62.4
PrFeAsO	1.76	57.2	18.2	3.4	1.57	93.6
NdFeAsO	1.49	42.1	15.2	−1.7	1.38	72.5
$CaFe_2As_2$	1.51	36.6	19.4	−2.8	0.95	75.4
$SrFe_2As_2$	1.69	42.0	16.0	2.6	1.31	74.0
$BaFe_2As_2$	1.68	43.0	14.3	−3.1	1.51	71.5
KFe_2As_2	1.58	42.5	15.0	−2.9	1.42	72.5
LiFeAs	1.69	43.4	22.9	−2.5	0.95	89.2

TABLE I: Calculated Fe moments (in μ_B) and in-plane exchange interactions (in meV), using experimental $z(As)$.

give smaller moments. The cases in which DFT overestimates magnetic moments are rare, and the cause is still under debate for Fe oxypnictides. Although some theorists suggest it is due to the frustrated magnetic structure [21], Mazin and Johannes suggest an alternative picture [40] based on magnetic fluctuation and inhomogenieties. Importantly the electronic structure features such as electron-hole symmetry and the exchange interaction strengths are better described with $z(As)_{exp}$ when compared to available experimental data [9, 26]. Thus our discussion will be based on the results from $z(As)_{exp}$. The sensitivity of moments and exchange interactions to $z(As)$ is large. For example, in LaFeAsO the change of $z(As)$ by $0.04\AA$ ($\Delta z(As) = 0.005$ in terms of internal coordinates) induces about 10% difference in the moment and up to 20% in the exchange interactions [29]. The same order of sensitivity was also reported for $CaFe_2As_2$ [30]. Therefore the deviation of up to 8% for moments and 30% for major exchange interactions (J_{1a} and J_2) are not significant, and become much smaller if $z(As)$ could be refined for each material. Taking this into account, we can say that the magnetic moments and exchange interactions are uniform throughout the materials considered here.

One of the most important quantities to understand the superconducting mechainsm in these materials is the ratio of $J_{1a}/2J_2$, which has so far not been measured nor calculated. According to the spin Hamiltonian studies [21, 22, 23], assuming Fe pnictides as magnetic Mott insulators like cuprates, at $J_{1a}/2J_2 \approx 1$ the system is close to the quantum critical regime, so superconducting ground state may appear as a result of the magnetic frustration and fluctuation [21, 22, 23, 41]. Note that the calculated ratios shown in Table I are all around unity. Therefore the universal behavior of $J_{1a}/2J_2$ suggests the magnetic fluctuation as the superconducting mechanism. Once again the deviations of $J_{1a}/2J_2$ from unity reflect not only the intrinsic material properties but also the sensitive dependence on $z(As)$. Although there is no apparent relation between the $J_{1a}/2J_2$ ratio and T_C, the universal feature of $J_{1a}/2J_2$ near unity is closely associated to superconductivity since it is present throughout the materials studied here, implying a spin-fluctuation-induced pairing mechanism [42].

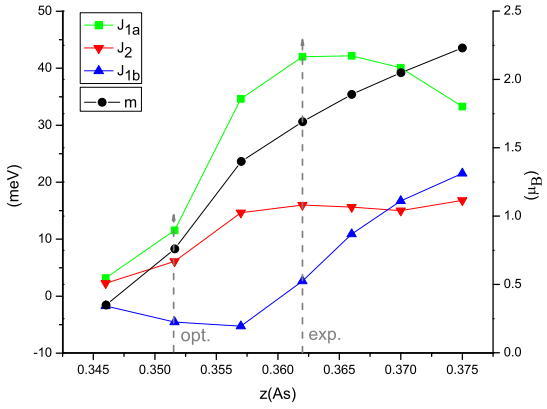

FIG. 3: (Color online) Calculated magnetic moments (solid circles) and exchange interactions (squares and triangles) vs. $z(As)$ for $SrFe_2As_2$.

Another important quantity is $|J_{1a}+2J_2|$ which determines the spin wave velocity in $(\pi, 0)$ direction, and can be directly probed by neutron scattering experiments. The available experimental data are in general agreement to our calculation. For $SrFe_2$ As_2 calculation shows $|J_{1a}+2J_2| = 74meV$, which is close to $100 \pm 20meV$ measured by neutron scattering [9]. Also, for $CaFe_2As_2$ our calculated $|J_{1a}+2J_2| = 75meV$ is slightly smaller than the measured $95 \pm 16meV$ [26] (derived from the observed spin wave velocity, see eq.(3) below). The fact that our calculated exchange constants are smaller than experimental ones (in both materials compared) is partially due to the built-in error of LSDA in predicting the z-position of As.

As an example, Fig. 3 shows the $z(As)$-dependence of the magnetic moments and interactions of $SrFe_2As_2$. The moment is a simple monatomic function of $z(As)$ ranging from $0.35\mu_B$ to $2.23\mu_B$. The three J's have different behaviors. J_{1a} increases drastically with $z(As)$ at the beginning, saturates in the middle, and eventually heads down. J_{1b} changes sign at $z(As)_{\rm exp}$, and eventually surpasses J_2. Also, J_{1a} and J_2 plateau in the small region around $z(As)_{exp}$. Similar behaviors are also found in other materials. Therefore the $J_{1a}/2J_2$ and $|J_{1a}+2J_2|$ values presented in Table I are robust against the small deviations in $z(As)$ around the experimental values. From the data one can also calculate $J_{1a}/2J_2$ vs. $z(As)$, which reveals the existence of the "sweet spot" where the optimal ratio $J_{1a}/2J_2 = 1$ is achieved. In the case of $SrFe_2As_2$ it is $z(As) = 0.357$.

The calculated spin wave dispersion gives more intuitive information about the magnetic interaction and anisotropy of these systems [9, 25]. The dispersion relation of the 2D (π, π)-AFM lattice reads

$$\omega_{\pm}(\mathbf{q}) = S\sqrt{|\mathcal{J}_0 \pm J_{1b}(\mathbf{q})|^2 - |J_{1a}(\mathbf{q}) \pm J_2(\mathbf{q})|^2}, \quad (1)$$

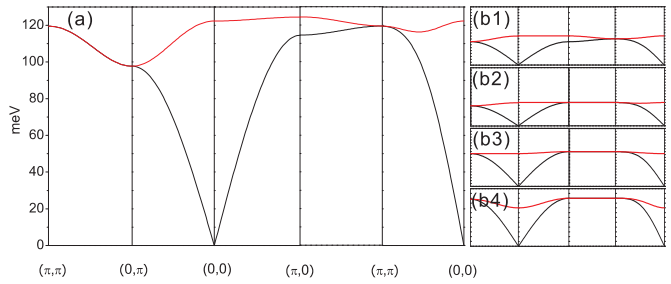

FIG. 4: (Color online) (a) The calculated spin wave dispersion of $SrFe_2$ As_2 along high-symmetry lines. (b) Spin waves dispersions with different sets of J's (arbitrary units), and $S = 1$ is fixed everywhere: (b1) $J_{1a} = -1$, $J_2 = -0.5$, $J_{1b} = 0.25$; (b2) $J_{1a} = -1$, $J_2 = -0.5$, $J_{1b} = 0$; (b3) $J_{1a} = -1$, $J_2 = -1$, $J_{1b} = 0$; (b4) $J_{1a} = -1$, $J_2 = -2$, $J_{1b} = 0$.

where

$$J_{1a}(\mathbf{q}) = 2J_{1a}e^{-iq_x}\cos q_x, \quad (2a)$$

$$J_2(\mathbf{q}) = 2J_2e^{-i(q_x+q_y)}[\cos(q_x+q_y)+\cos(q_x-q_y)], \quad (2b)$$

$$J_{1b}(\mathbf{q}) = 2J_{1b}e^{-iq_y}\cos q_y, \quad (2c)$$

$$\mathcal{J}_0 = 2J_{1a}+4J_2-2J_{1b}. \quad (2d)$$

$\omega_-(\mathbf{q})$ is an optical mode with non-zero frequency at $(0,0)$ point, which is mainly associated with high energy excitations and thus hard to measure by neutron experiments. Using the calculated magnetic exchange constants, we plot the spin wave dispersion of $SrFe_2As_2$ in Fig. 4 (left panel), whose $S = 0.94$ is taken from experiment [8]. The non-symmetric dispersions in $(0,0)-(0,\pi)$ and $(0,0)-(\pi,0)$ directions indicate in-plane magnetic anisotropy, which is a major difference from cuprates. At small q near $(0,0)$, the spin wave velocity in the $(\pi,0)$ direction is

$$v_\perp = aS\,|2J_{1a}+4J_2|\,, \quad (3)$$

which is the relation used to experimentally determine $|J_{1a}+2J_2|$, such as for $SrFe_2As_2$ [9]. To see how the three J's affect the dispersion, we also plot hypothetical spin waves using four sets of J's in the right panel of Fig. 4. $S = 1$ and $J_{1a} = 1$ are fixed, J_{1b} is set to be zero except in (b1), and J_2 varies from -0.5 to -2. It is clear that J_2 controls the energy scale of the spin wave, and J_{1b} produces the small dispersion within the $(\pi,0)-(\pi,\pi)$ panel. The difference in J_{1a} and J_{1b}, a direct consequence of the Q_M-AFM ordering that breaks in-plane symmetry, accounts for the anisotropy in $(\pi,0)$ and $(0,\pi)$ directions. These anisotropic spin waves can be directly probed by neutron scattering experiments.

To conclude, we have studied the magnetic exchange interactions in the various Fe-based high T_C superconductors using first-principle based linear response calculations. From the nine different materials, the magnetic interactions are short-range and can be well described by the first and second nearest-neighboring interactions. Importantly $J_1/2J_2$ is close to unity for all the cases, which corresponds to the frustration limit. Calculated spin wave dispersions show the magnetic anisotropy and the roles of the three in-plane exchange interactions. Our result strongly suggests the magnetic fluctuation as the pairing mechanism for the superconducting ground state.

The authors acknowledge support from NSF Grants DMR-0606498 (S.Y.S) and DMR-0421810 (W.E.P), and collaborative work supported by DOE SciDAC Grants SE-FC0206ER25793 and DE-FC02-06ER25794.

[1] Y. Kamihara *et al.*, J. Am. Chem. Soc. **130**, 3296 (2008).
[2] X. H. Chen *et al.*, Nature **453**, 761 (2008).
[3] Z. A. Ren *et al.*, Chinese Phys. Lett. **25**, 2215 (2008).
[4] J. H. Tapp *et al*, Phys. Rev. B **78**, 060505(R) (2008).
[5] C. Krellner *et al.*, Phys. Rev. B **78**, 100504(R) (2008).
[6] A. Jesche *et al.*, arXiv:0807.0632 (2008).
[7] A. I. Goldman *et al.*, Phys. Rev. B **78**, 100506(R) (2008).
[8] J. Zhao *et al.*, Phys. Rev. B **78**, 140504(R) (2008).
[9] J. Zhao *et al.*, Phys. Rev. Lett. **101**, 167203 (2008).
[10] L. Zhao *et al.*, arXiv:0807.0398 (2008).
[11] F. -C. Hsu *et al.*, PNAS **105,** 14262 (2008).
[12] M. H. Fang *et al.*, arXiv:0807.4775 (2008).
[13] K. -W. Yeh *et al.*, Europhysics Lett. **84,** 37002 (2008).
[14] Y. Mizuguchi *et al.*, Appl. Phys. Lett. **93**, 152505 (2008).
[15] L. Boeri, O. V. Dolgov and A. A. Golubov, Phys. Rev. Lett. **101**, 026403 (2008).
[16] K. Haule, J. H. Shim and G. Kotliar, Phys. Rev. Lett. **100**, 226402 (2008).
[17] A. J. Drew et al, Phys. Rev. Lett. **101**, 097010 (2008).
[18] W. Bao *et al.*, arXiv:0809.2058 (2008).
[19] J. J. Pulikkotil, M. van Schilfgaarde, and V. P. Antropov, arXiv:0809.0283 (2008).
[20] F. Ma *et al.*, arXiv:0809.4732 (2008).
[21] Q. Si and E. Abrahams, Phys. Rev. Lett. **101**, 076401 (2008).
[22] C. Fang *et al.*, Phys. Rev. B **77**, 224509 (2008).
[23] C. Xu, M. Müller, and S. Sachdev, Phys. Rev. B **78**, 020501 (2008).
[24] J. Wu, P. Phillips, and A. H. Castro Neto, Phys. Rev. Lett. **101**, 126401 (2008).
[25] G. S. Uhrig *et al.*, arXiv:0810.3068 (2008).
[26] R. J. McQueeney et at, arXiv:0809.1410 (2008).
[27] A. Georges *et al.*, Rev. Mod. Phys. **68**, 13 (1996).
[28] G. Kotliar *et al.*, Rev. Mod. Phys. **78**, 865 (2006).
[29] Z. P. Yin *et al.*, Phys. Rev. Lett. **101**, 047001 (2008).
[30] T. Yildirim, Phys. Rev. Lett. **101**, 057010 (2008).
[31] K. Kuroki *et al.*, Phys. Rev. Lett. **101**, 087004 (2008).
[32] C. Cao, P. J. Hirschfeld, and H.-P. Cheng, Phys. Rev. B

77, 220506 (2008).
[33] K. Nakamura, R. Arita, and M. Imada, J. Phys. Soc. Jpn. **77**, 093711 (2008).
[34] E. Manousakis *et al.*, arXiv:0806.3432 (2008).
[35] D. J. Singh and M.-H. Du, Phys. Rev. Lett. **100**, 237003 (2008).
[36] A. I. Liechtenstein *et al.*, J. Magn. Magn. Mater. **67,** 65 (1987); P. Bruno, Phys. Rev. Lett. **90,** 087205 (2003).
[37] X. Wan, Q. Yin, and S. Y. Savrasov, Phys. Rev. Lett. **97,** 266403 (2006).
[38] M. J. Han, X. Wan, and S. Y. Savrasov, Phys. Rev. B **78,** 060401(R) (2008).
[39] S. Y. Savrasov, Phys. Rev. B **54,** 16470 (1996).
[40] I. I. Mazin and M. D. Johannes, arXiv:0807.3737 (2008).
[41] A. V. Chubukov, D. Efremov and I. Eremin, Phys. Rev. B **78**, 134512 (2008).
[42] T. Moriya, Proc. Jpn. Acad. Ser. B **82**, 1 (2006).